2016

An Experimental Study on the Effect of a new Defrosting Strategy on the Energy Consumption of Household Refrigerators

Fernando Testoni Knabben
Federal University of Santa Catarina, Brazil, fernandok@polo.ufsc.br

Claudio Melo
Federal University of Santa Catarina, Brazil, melo@polo.ufsc.br

An Experimental Study on the Effect of a New Defrosting Strategy on the Energy Consumption of Household Refrigerators

Fernando T. KNABBEN[1], Cláudio MELO[1]*

[1]POLO – Research Laboratories for Emerging Technologies in Cooling and Thermophysics
Department of Mechanical Engineering, Federal University of Santa Catarina, Florianópolis, SC, Brazil,
+55 48 3234 5691, melo@polo.ufsc.br

* Corresponding Author

ABSTRACT

In a previous study, an experimental testing apparatus was constructed and used to measure the defrosting efficiency of different heaters working under different control strategies. Based on the obtained results two types of heaters (calrod and distributed) and two power modes (integral and steps) were selected for this study. In the integral mode, the power was held at 160 W and the defrosting period set to 17.0 and 19.3 min for the distributed and calrod heaters, respectively. Conversely, in the steps mode, the power was gradually reduced from 160 to 20 W and the defrosting period set to 28.5 and 22.3 min for the distributed and calrod heaters, respectively. The energy consumption of a typical top-mount frost-free refrigerator running with the four combinations of heater and control mode was measured following both the ISO and AHAM standards. Changes were made in the product electronic board to vary the power and time of the steps. A glass window was also installed in the rear wall of the refrigerator to visually monitor the defrosting process. A 4.3 % drop in the energy consumption was achieved when the pair calrod heater/integral mode was replaced by the pair distributed heater/steps mode, independently of the standard used. Clogging tests were also carried out to check the robustness of the different defrosting strategies.

1. INTRODUCTION

Frost-free refrigerators are mostly assembled with forced-draft tube-and-fin evaporators. Particularly, in a two-compartment refrigerator, a large part of the circulating airflow is directed to the freezer, while the remainder is blown into the fresh-food compartment. The infiltration of hot and humid air due to periodic door openings and through the door gaskets directly affects the psychrometric conditions inside the compartments, especially in the fresh food compartment. The cold evaporator surfaces are thus reached by two air streams with distinct humidity ratios, giving room for a non-uniform frost distribution.

Frost is essentially a porous medium formed by the desublimation of the water vapor contained in an air stream (Knabben *et al*., 2011). The accumulation of frost decreases the cooling capacity and the overall performance of the refrigerator. This is so not only because the frost layer acts as a thermal insulator but also because it increases the air side pressure drop, thereby decreasing the fan-supplied airflow rate. Thus, frost is periodically removed from the evaporator surfaces, usually through electrical heaters. However, during defrosting the compressor and the fan are both turned off. Moreover, only a small fraction of the heat released by the heater is effectively used for melting the frost (Niederer, 1986), with the rest contributing to an increase in the internal thermal load. Consequently, to balance this extra load the compressor runtime after defrosting is longer. Additionally, the defrost heater itself increases the air side pressure drop, leading to an even lower airflow rate. Thus, it is clear that the defrosting process, although necessary, adversely affects the refrigerator performance.

In larger refrigeration systems defrosting is usually carried out through the hot-gas and reverse cycle techniques (Stoecker, 1984, Cho *et al*., 2005, Byun *et al*., 2008, Dopazo *et al*., 2010, Minglu *et al*., 2010, Dong *et al*., 2012). In the hot-gas technique vapor from the compressor discharge is directed to the evaporator, while in the reverse cycle

method the refrigeration cycle is reversed by a four-way valve. However, these techniques are not typical in domestic appliances, where electrical heaters are dominant due to simplicity and cost issues.

Few studies on defrost heaters have been reported in the literature: Kim *et al*. (2006), Bansal *et al*. (2010), Ozkan *et al*. (2012) and Knabben *et al*. (2011). Kim *et al*. (2006) compared different defrost heaters using a side-by-side refrigerator, but provided no information on the operating conditions and how they were controlled. Bansal *et al*. (2010) studied the heat distribution from a calrod heater to the different parts of an upright freezer. A mathematical model has been proposed to predict this distribution, and it was found that only 32% of the heat was actually used to melt the frost. Ozkan *et al*. (2012) experimentally analyzed the evaporator defrost using a dual-compartment refrigerator with a distributed heater. The authors, however, removed the mullion, changing the nature of the original internal air distribution. With the aid of an endoscopic camera, they noted that the frost accumulates mostly in the first rows of the evaporator, suggesting that most of the power should be released in this area. This observation corroborates the conclusions of Knabben *et al*. (2011), who tested the same type of heater in a similar refrigerator. Knabben *et al*. (2011) also found that the gradual reduction of the defrost power during defrosting can increase the process efficiency.

This study focuses on a comparison between different heaters and defrosting modes. The study was divided into two phases. In the first phase, whose results were previously published by Melo *et al*. (2013), an auxiliary refrigeration loop was attached to a refrigerator to provide the desirable operating conditions. Additionally, the compartment temperatures were kept constant and water vapor was generated internally to provide the same frost mass for all tests. A systematic comparison was carried out based on the so-called defrosting efficiency. In the second phase, the aim was to correlate the defrosting efficiency with the energy consumption of the refrigerator. To this end, two heaters and two strategies (of the three analyzed in phase 1) were selected and cyclic energy consumption and door-opening tests were carried out.

2. EXPERIMENTAL WORK

2.1 Phase 1

In the first phase of this study (Melo *et al*., 2013) an experimental apparatus was built specifically to emulate the typical operating conditions of a frost-free refrigerator. The apparatus was comprised of an auxiliary refrigeration loop, the cabinet of a top-mount 263-liter refrigerator, a water vapor generating system and a climate chamber. The original circuit of the refrigerator was removed (except for the evaporator) and replaced by the auxiliary loop. The loop allowed the evaporating temperature to be controlled by varying the condenser PID-driven fan speed. During all tests the evaporator was kept flooded, i.e., without superheating. The evaporating temperature was assumed to be equal to the average temperature of the tubes, measured with 10 T-type thermocouples installed along the coil, and it was held at -23 ºC. In order to speed up the frost accumulation process, water vapor was released into the fresh-food compartment with the aid of an electrical heater immersed in a water reservoir. The power of the heater was also controlled by a PID-controller, the action of which was based on the signal sent by a relative humidity sensor placed in the center of the compartment. The relative humidity was maintained at 90 %. The air temperatures in the freezer and fresh-food compartments were controlled with electrical heaters distributed inside the cabinet and held at -18 and 5 ºC, respectively. The ambient temperature was kept at 25 ºC. Each test lasted 9 h. The defrosted water was collected and weighted after each test. The end of the defrosting period was determined based on both visual inspection of the evaporator and the water mass collected. In order to visualize the frosting and defrosting processes, an insulating 40-mm-thick glass window was installed in the freezer rear wall.

Eleven tests were performed to measure the efficiency of three different defrost heaters: distributed, calrod and glass tube, with nominal powers of 160, 300 and 160 W, respectively (see Figure 1). The distributed heater has four tubes (5 mm diameter and 380 mm length) on each side of the evaporator and is in direct contact with the fins. The calrod heater has only one tube (5 mm diameter and 380 mm length) placed below the evaporator. Likewise, the glass tube heater is comprised of a single tube (10mm diameter and 310 mm length) and is also installed under the evaporator. Both the calrod and glass tube heaters dissipate heat mostly by natural convection and radiation, while the distributed heater releases heat basically through conduction. Additionally, three operating modes were tested: integral, steps and pulsating power (see Figure 2). The aim was to analyze the effect of different time and power combinations on the defrosting efficiency. The first mode (integral) is the simplest and the most common in real applications. In this case, the heater is kept on, at the nominal power, during the whole process. The second mode

(steps) consists of gradually reducing the power over time (since the defrost energy is a function of the frost mass, and the mass decreases during the process, it is expected that the defrost efficiency will increase with a power reduction). The third mode (pulsating) follows the same lines: power modulation during defrosting. In this case, the heater works in an on-off cyclic behavior, at the nominal power. Table 1 shows all of the power and time combinations. Other parameters were also evaluated: heater maximum temperature, T_h, freezer average temperature after defrosting, T_{fz}, evaporator coil average temperature after defrosting, T_w, and frost mass, m. The distributed heater temperature was measured at two points (central tube and bottom tube), while the calrod and glass tube temperatures were measured only in the middle of the tube. Due to experimental issues, the heater temperature was not measured in the first three tests. The defrost efficiency, η_d, was calculated, with an average uncertainty of ±2.5 %, through the following equation:

$$\eta_d = \frac{mc_{p,i}\left(T_{melt} - T_w\right) + mh_{sl}}{\int_0^t W_d\, dt} \tag{1}$$

where t and W_d are the defrost time and power, respectively, $c_{p,i}$ is the ice specific heat (~1.9 kJ/kgK) and T_{melt} and h_{sl} are, respectively, the water fusion temperature (0 ºC) and the latent heat (~333.6 kJ/kg).

Figure 1: Defrost heaters: (a) distributed, (b) glass tube, (c) calrod (Melo *et al.*, 2013)

The first test was conducted with the distributed heater operating in the integral mode during 20 min. It was found that all frost had been removed after approximately 15 min. Thus, the mass collected in this test (~155 g) was considered as a reference to be held for the following tests. The second test was carried with the distributed heater also operating in the integral mode but with no time constraint. It was noted that after 15.2 min the heater had melted the frost and that the evaporator coil average temperature reached 0ºC after 8 min. The steps operating mode was then established by considering an initial period of 8 min, where the power was kept at the nominal value, and dividing the remaining time into 40-W steps, 2 min intervals. An analogous procedure was adopted for the calrod and glass tube heaters, where 3 and 2 min intervals were applied, respectively. However, since the defrosting time of the integral and steps modes are not identical, the steps adopted were not enough to completely melt the frost, and so the time of the last step needed to be extended (see Figure 2). Nevertheless, as shown in Table 1, the defrost efficiency increased in all cases when the steps mode was used. To define the time of the power pulses, the same procedure was adopted.

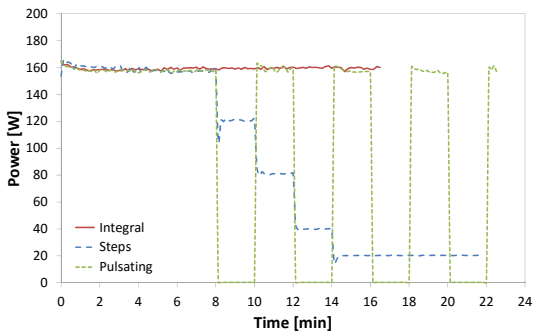

Figure 2: Defrost strategies: tests 5, 8 and 11

Tests 3 and 4 were carried out with the calrod heater also operating in the integral mode but with two power levels: 300 W (nominal power) and 160 W (as in the case of the distributed heater). As expected the defrosting efficiency of test 3 was lower than that of test 2. The power almost doubled in test 3, which explains the shorter defrosting time. However, most of the heat was transferred to the surroundings and not to the frost layer. It was also noted that the defrosting efficiency of test 4 was lower than that of test 2, which means that for the same power a shorter time was required for the distributed heater to complete the process. It was also found that the efficiency of the glass tube heater/integral mode (test 5) was similar to that provided by the distributed heater/integral mode (test 2). It should be pointed out that both the calrod and glass tube heaters reached temperatures above 300 ºC, thereby demanding safety precautions.

High heater temperatures were also recorded in tests 7 and 8, with the calrod and glass tube heaters, respectively. The distributed heater, however, remained at below 100 ºC (test 6). As the heater power decreases with time, the heating of the parts next to the evaporator is minimized, which is an advantage of the steps mode. The pulsating mode was analyzed in tests 9 to 11. As can be noted, the defrosting time of the distributed heater operating in the pulsating mode was longer than that found with the integral mode. This explains the higher temperature within the freezer compartment after defrosting. Despite reaching high temperatures during the initial transient, the heater temperatures were considerably reduced during the cycling period.

Of the three operating modes investigated in this study, the steps mode was found to be the most efficient. However, both the defrosting time and freezer temperature after defrost were higher when compared to the integral mode. The calrod and glass tube heaters did not heat the freezer during defrosting (as observed with the distributed heater), but as they reach very high temperatures some heating is expected when the fan start again after defrosting. Thus, even though the previous tests indicated a possible increase in the defrosting efficiency through changes in the dissipation time and power, the contribution of this increase to a reduction in the energy consumption of a refrigerator is not yet known. In this context, cyclic tests were performed according to the standards ISO 8561 (1995) and AHAM HFR-1 (2008). Additionally, in order to check the process robustness, cyclic tests with periodic door openings were also conducted.

Table 1: Phase 1 experimental results (Melo *et al.*, 2013)

Test	Heater	Mode	t [min]	W_d [W]	T_h [°C]	T_{fz} [°C]	T_w [°C]	m [g]	η_d [%]
1	Distributed	Integral	19.6	160	-	-9.2	23.1	155.2	31.1
2	Distributed	Integral	15.2	160	-	-13.6	12.9	149.0	38.6
3	Calrod	Integral	11.9	300	-	-14.8	22.3	153.2	27.5
4	Calrod	Integral	19.3	160	343.4	-11.8	16.4	155.1	34.0
5	Glass tube	Integral	16.8	160	354.1	-13.3	9.5	152.0	36.0
6	Distributed	Steps	28.5	160 to 20	73.8	-5.8	4.3	157.1	45.7
7	Calrod	Steps	22.3	160 to 20	288.9	-10.0	6.8	149.9	43.4
8	Glass tube	Steps	21.9	160 to 20	340.5	-11.2	2.2	147.4	48.0
9	Distributed	Pulsating	22.9	160 or 0	70.4	-8.9	9.3	154.8	39.9
10	Calrod	Pulsating	23.2	160 or 0	278.6	-10.0	9.6	155.7	42.7
11	Glass tube	Pulsating	22.6	160 or 0	340.8	-10.5	5.0	146.2	39.8

2.1 Phase 2

The main objective of this phase was to investigate the impact of the defrosting efficiency on the energy consumption of a particular model of refrigerator. To this end, the refrigerator used before was also used in this phase. However, both the damper - the device that modulates the airflow rate between the compartments - and the thermostat - the sensor that sets the compressor runtime - were reactivated. Thus, the original operating logic of the refrigerator was reestablished. The defrost onset time was determined by the refrigerator electronic board, but the defrost offset time and strategy were pre-determined, i.e., the defrost terminator, which is originally installed at the evaporator outlet, was deactivated. A parallel logic was developed to avoid the compressor and fan coming on before the defrosting ends (something that could occur according to the original logic).

Cyclic energy consumption tests were carried out according to the ISO 8561 (1995) and AHAM HFR-1 (2008) standards. According to these standards, the refrigerator must be tested in a room kept at approximately 32 ºC. The AHAM standard establishes reference temperatures of -17.9 and 3.9 ºC for the freezer and fresh-food compartments,

respectively. Conversely, the ISO standard establishes reference temperatures of -18 ºC and 5 ºC. The main difference between the standards is the thermal packages used only in the ISO tests (Hermes *et al.*, 2013). Some of these packages, called M-packages, are instrumented with thermocouples and the warmest one is used as the reference for the freezer compartment. The reference temperature for the fresh-food compartment is the average value of three packages placed in the geometric center of the compartment: top, middle and bottom. In general, in both standards, the tests cover two defrosting periods. Additionally, two tests were carried out - one above (cold) and another below (warm) the compartment reference temperatures - , for each pair of heater and control mode. The energy consumption was obtained through a linear interpolation based on the two tests.

Of the heaters used in phase 1 only two were selected for phase 2: distributed and calrod. The glass tube heater was discarded because its use is restricted to a few countries. From the previous defrost strategies the integral and steps modes were chosen: the integral mode because it is the most commonly used and it will serve as a basis for comparison; and the steps mode because it was found to be the most promising one. In the integral mode, both distributed and calrod heaters were tested with the same power (160 W), but with defrosting periods of 17.0 and 19.3 min, respectively. A defrosting period of 17.0 min (and not 15.2 min, as shown in Table 1) was used with the distributed heater because this is the original setting of the refrigerator. For the steps mode logics of tests 6 and 7 (see Table 1) were adopted.

In addition to the overall energy consumption (EC_t), others parameters were also object of this study, such as the fraction of the defrost energy consumption over the overall energy consumption (EC_d), the runtime ratio of the first cycle after defrost (RTR), the fraction of the energy consumption of the first cycle after defrost over the overall energy consumption (EC_{c1}) and the evaporator and refrigerated compartments temperatures during the defrost period. An extra parameter, called EC_{dr}, which denotes the fraction of the defrost plus the recovery period energy consumption (ISO 8561, 1995) over the overall energy consumption, was also considered. Some of these parameters are illustrated in Figures 3 and 4, for the distributed heater operating in the integral mode.

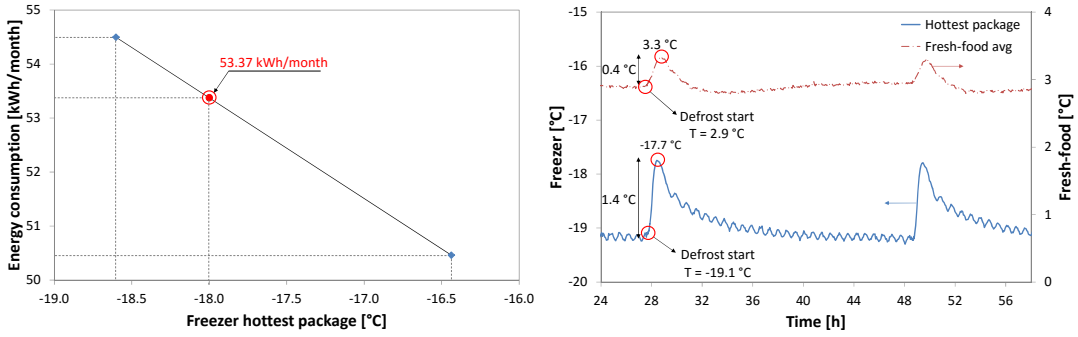

Figure 3: Energy consumption interpolation (left) and compartment temperatures (right)

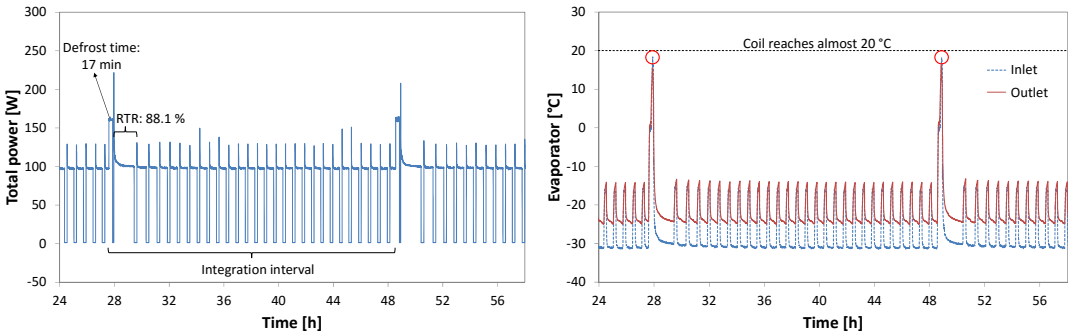

Figure 4: Power and runtime (left) and evaporator coil temperature (right)

Table 2 shows the results of the ISO tests for each combination of heater and operating mode. It can be noted that temperatures higher than 5ºC in the fresh-food compartment were not reached in any of the warm tests. The energy consumption was then interpolated considering only the freezer reference temperature (ISO 8561, 1995).

Table 2: Phase 2 experimental results

Parameter	Distributed/Integral (17.0 min)		Distributed/Steps (28.5 min)		Calrod/Integral (19.3 min)		Calrod /Steps (22.3 min)	
	Cold	Warm	Cold	Warm	Cold	Warm	Cold	Warm
Freezer - warmest pack, ºC	-18.6	-16.4	-20.2	-17.4	-18.5	-16.3	-18.8	-16.5
Fresh-food max avg., ºC	3.0	2.5	2.9	2.0	4.8	3.4	4.9	3.5
RTR, %	88.1	75.9	89.2	84.2	93.2	83.9	92.0	82.0
Freezer max, ºC	-17.7	-15.8	-18.9	-16.5	-16.8	-15.3	-17.5	-15.5
Freezer ΔT, ºC	1.4	1.0	2.5	1.6	2.5	1.8	1.8	1.6
Fresh-food max, ºC	3.3	2.7	3.3	2.5	5.5	3.8	5.5	4.0
Fresh-food ΔT, ºC	0.4	0.3	0.6	0.5	0.8	0.5	0.7	0.7
Evaporator max, ºC	22.0	22.2	1.3	5.6	19.2	22.3	5.1	6.3
EC_d, %	1.4	1.3	1.1	1.1	3.3	3.2	2.3	2.3
EC_{c1}, %	4.8	4.7	5.2	4.8	11.8	12.3	9.8	9.8
EC_{dr}, %	11.7	11.6	10.7	10.9	23.8	23.6	22.3	21.7
EC_t, kWh/month	54.49	50.46	55.05	51.73	55.13	53.5	54.33	51.30
	53.37		52.39		54.74		53.29	

An analysis of the distributed heater results shows that a reduction in the energy consumption of 1.8 % was achieved when the steps mode was used. The contribution of the defrost energy consumption to the overall energy consumption was also reduced, since the steps mode provides a better use of the dissipated energy. Consequently, the evaporator maximum temperature dropped by nearly 20 ºC. Despite the longer defrosting period, the runtime of the first cycle after defrosting was not affected significantly. However, the fraction of the defrost plus the recovery period energy consumption over the overall energy consumption, reduced almost 1.0 %. A summarized comparison of the EC and EC_{dr} parameters is shown in Figure 5.

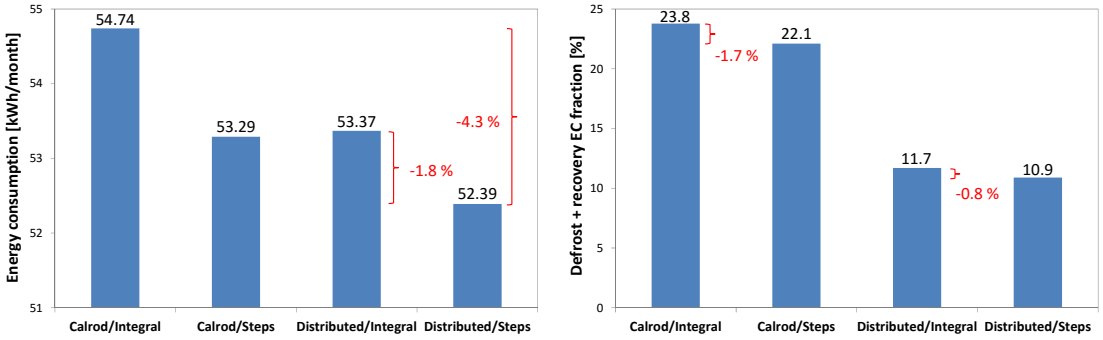

Figure 5: Total consumption (left) and defrost + recovery period consumption fraction (right)

The same analysis was applied to the calrod heater and once gain it was observed that the contribution of the defrost power to the overall energy consumption was lower when the steps mode was adopted. The maximum temperature of the evaporator was also considerably lower. In addition, the temperature rise inside the compartments due to defrosting with the steps mode was similar to that observed with the integral mode. A slight reduction in the energy consumption of the first cycle after defrosting was also noted. The combination of such factors contributed to a reduction of 2.6 % in the overall energy consumption.

In general, the performance of the **c**alrod heater is poorer than that of the distributed heater regarding the energy consumption. Even in the steps mode, the energy consumption of the refrigerator tested with the calrod heater was nearly the same as that observed for the distributed heater in the integral mode. On comparing the two heaters operating in the integral mode, it can be observed that the temperature rise inside the compartments due to defrosting is higher with the calrod heater. This, to some extent, was expected, not only because the calrod heater reaches temperatures that are almost three times higher than those of the distributed heater but also because of its design and relative position in respect to the evaporator. According to the manufacturer, this model of refrigerator is mounted with the distributed or the calrod heater depending on where it is sold. Energy savings of 4.3% can then be achieved by replacing the pair calrod heater/integral mode by the pair distributed heater/steps mode.

Since the same refrigerator model is manufactured in different regions of the globe, it must be tested according to the current standards of each region. Therefore, additional energy consumption tests were carried out following the AHAM HFR-1 (2008) standard. These tests also served to validate the results obtained with the ISO 8561 (1995) standard. Figure 6 compares the defrost effect on the compartment temperatures for both the ISO and AHAM standards, considering the cold test of the calrod heater in the steps mode. It is worth noting that the temperature of both compartments rises considerably when the test is carried out according to the AHAM standard. The absence of packages considerably reduces the thermal inertia of the compartments, increasing their sensitivity to the internal thermal load. However, this sudden rise in the temperature did not translate into a considerable increase in the energy consumption, because the compressor runtime ratio after defrosting (86.6 %) was close to that of the ISO test (91.2 %). This means that since the compartments warm up rapidly due to the lower inertia, they cool down at almost the same rate.

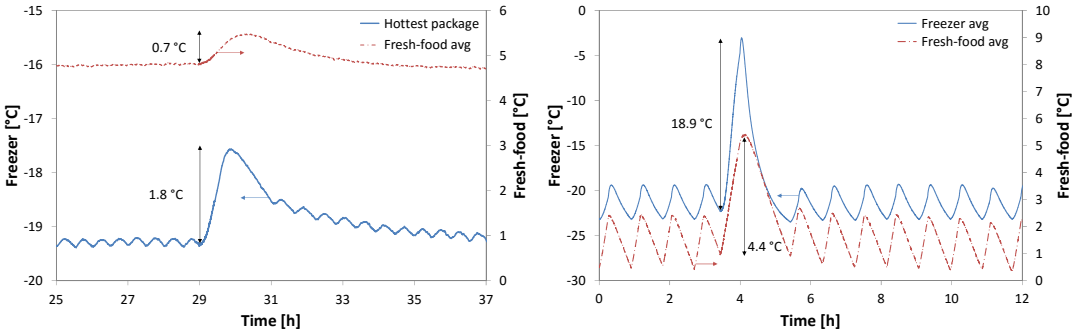

Figure 6: Defrost effect on compartment temperatures for ISO (left) and AHAM (right) standards: calrod, steps

To sum up, the results obtained with the AHAM standard followed the same trends observed with the ISO standard. Clearly, due to the absence of packages in the freezer, the air side pressure drop was lower and therefore the airflow rate was higher. Thus, the AHAM energy consumption values were lower. However, as shown in Figure 7, the trends are almost parallel, which validates the results obtained with the ISO standard. It should be noted that for the AHAM warm tests it was possible to reach temperatures higher than 3.9 ºC in the fresh-food compartment, which also allowed the interpolation of the energy consumption for this compartment. The final energy consumption, in this case, was considered to be the highest of the interpolated values for each compartment.

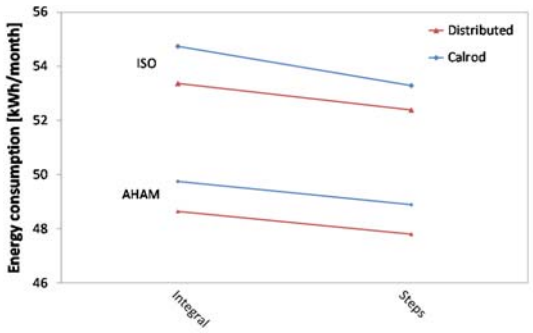

Figure 7: Comparison between ISO and AHAM interpolated energy consumptions

In order to check the robustness of each defrosting strategy, additional cyclic tests without loading packages were performed with the aid of an automatic door-opening device (Piucco *et al.*, 2011), shown in Figure 8. During the tests the ambient temperature and relative humidity were kept at 32 ºC and 85 %, respectively. In order to provide a more intense frost accumulation, the refrigerator was submitted to the following door-opening routine defined by the manufacturer: freezer door opened at a 90º angle for 15 s and totally closed for 30 min, and fresh-food compartment door also opened 90º for 15 s, but closed for 10 min. This routine was repeated continuously for 24 h. During each test two defrosts were carried out. To avoid excessive condensation on the glass window (caused by the high ambient humidity) and to improve the visualization, an acrylic cover was installed next to the freezer rear wall. A

high-definition webcam was installed to visualize the process and silica packages were placed inside the plastic cover, also to avoid the possibility of internal fogging. The window was lit indirectly with led lamps to prevent reflections on the glass and to minimize the thermal load.

Figure 8: Door-opening device (left) and visualization improvement (right)

Figure 9 shows a sequence of photos taken at four distinct moments during the test with the distributed heater operating in the steps mode. The first photo (Figure 9a) shows the evaporator before the start of the door-opening routine. It can be noted that the evaporator was practically dry. The second photo (Figure 9b) shows the evaporator immediately before the beginning of defrosting, which started around 8 h after the beginning of the periodic door-openings. It is worth noting that the frost accumulation was considerable and that the evaporator was practically clogged near the central region between the first and fifth rows. Figure 9c was taken right after defrosting and it was observed that almost all of the frost mass had melted, with only a small amount remaining in the middle of the evaporator, close to the fifth row. It is important to note that there are no heater tubes in this region. The last photo (Figure 9d) was taken minutes after the defrosting had ended, during the interval where the compressor was still off. It can be seen that the residual frost was almost completely removed due to the lack of refrigeration in this period and to some existing heating. This behavior was also observed with the calrod heater in both operating modes and with the distributed heater in the integral mode.

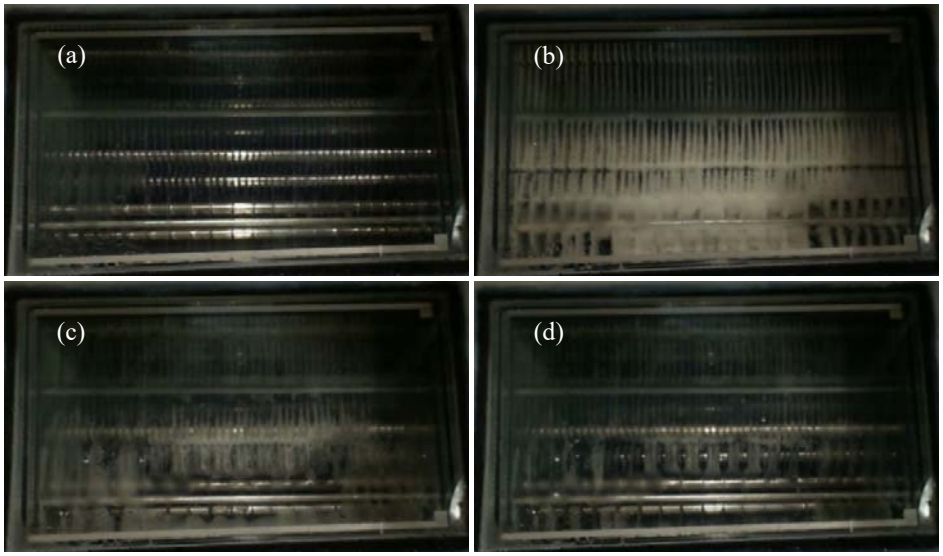

Figure 9: Defrost visualization: Door-opening test with distributed heater in steps mode

6. CONCLUSIONS

The effect of different heaters and defrosting strategies on the energy consumption of a household refrigerator was investigated. In a first phase, the results provided by a testing apparatus showed that the defrosting efficiency of any type of heater is considerably improved when the conventional integral control mode is replaced by a new control strategy, called steps mode. In a second phase, the original cycle and the electronic board of the refrigerator were reinstalled and cyclic energy consumption tests were carried out according to the ISO 8561 (1995) and AHAM HRF-1 (2008) standards. It was found that the relationship between defrosting efficiency and energy consumption is not linear. For instance, when the calrod heater operating mode was changed from integral to steps, the defrosting efficiency increased from 34.0 to 43.4 %, which translates into a drop in energy consumption of 2.6 %. It was also found that the distributed heater consumes less energy than the calrod heater and that a reduction of 4.3 % can be achieved by replacing the calrod heater in the integral mode with the distributed heater in the steps mode.

REFERENCES

AHAM HRF-1. (2008). Energy Performance and Capacity of Household Refrigerators, Refrigerator-freezers and Freezers. American National Standards Institute, Washington-DC, USA.

Byun, J. S., Lee, J., & Jeon, C. D. (2008). Frost retardation of an air-source heat pump by the hot gas bypass method. *Int. J. Ref.*, *31*(2), 328–334.

Bansal, P., Fothergill, D., & Fernandes, R. (2010). Thermal analysis of the defrost cycle in a domestic freezer. *Int. J. Ref.*, *33*(3), 589–599.

Cho, H., Kim, Y., & Jang, I. (2005). Performance of a showcase refrigeration system with multi-evaporator during on-off cycling and hot-gas bypass defrost. *Energy*, *30*(10), 1915–1930.

Dong, J., Deng, S., Yiqiang, J., Liang, X., & Yao, Y. (2012). An experimental study on defrosting heat supplies and energy consumptions during a reverse cycle defrost operation for an air source heat pump. *Applied T. Eng.*, *37*, 380–387.

Dopazo, J. A., Seara, J. F., Uhía, F. J., & Diz, R. (2010). Modelling and experimental validation of the hot-gas defrost process of an air-cooled evaporator. *Int. J. Ref.*, *33*(4), 829–839.

Hermes C. J. L., Melo C., & Knabben F. T. (2013). Alternative test method to assess the energy performance of frost-free refrigerating appliances. *Applied T. Eng.*, *50*(1), 1029–1034.

ISO 8561. (1995). Household frost-free refrigerating appliances – Refrigerators, refrigerator-freezers, frozen food storage cabinets and food freezers cooled by internal forced air circulation – Characteristics and test methods. Geneva, Switzerland.

Kim, Y., Tikhonov, A., Shin Y., & Lee, J. (2006). Experimental study on high performance defrosting heater for household refrigerator. *Proceedings of the 13th International Heat Conference*, Sydney, Australia.

Knabben, F. T., Hermes, C. J. L., & Melo C. (2011). Numerical and experimental investigation of the frosting and defrosting processes in no-frost evaporators. *Proceedings of the XI Congress of Refrigeration and Air Conditioning – CIAR2011*, Mexico City, Mexico.

Melo, C., Knabben, F. T. & Pereira, P. V. (2013). An experimental study on defrost heaters applied to frost-free refrigerators. *Applied T. Eng.*, *51*(1-2), 239–245.

Minglu, Q., Liang, X., Deng, S., & Yiqiang, J. (2010). Improved indoor thermal comfort during defrost with a novel reverse-cycle defrosting method for air source heat pumps. *Building and Environment*, *45*(11), 2354–2361.

Niederer, D.H. (1986). Frosting and defrosting effects on coil heat transfer. *ASHRAE Transactions*, *82*(1), 467–473.

Ozkan, D. B., Ozil, P., & Inan, C. (2012). Experimental investigation of the defrosting process on domestic refrigerator finned tube evaporators. *Heat T. Eng.*, *33*(6), 548–557.

Piucco R. O., Hermes, C. J. L., & Melo, C. (2011). In-situ evaluation of a criterion to predict frost formation on liners of refrigerated cabinets. *Applied T. Eng.*, *31*(14-15), 3084–3091.

Stoecker, W. F., 1984. Selecting the size of pipes carrying hot gas to defrost evaporators. *Int. J. Refrig.*, *7*(4), 225–228.

ACKNOWLEDGEMENTS

This study was made possible through the financial investment from the EMBRAPII Program (POLO/UFSC EMBRAPII Unit - Emerging Technologies in Cooling and Thermophysics). The authors thank Mr. Jean R. Backer for his support in the experiments and Whirlpool S.A. for financial and technical support.